

TRANSFER PROCESSES IN LOW-TEMPERATURE PLASMA

ON THE FORMATION OF CARBON NANOSTRUCTURES ON THE STEEL SURFACE OF A REACTOR AS A RESULT OF THE DECOMPOSITION OF HYDROCARBONS IN THE LOW-TEMPERATURE PLASMA.

1. EXPERIMENTAL SETUP, DETERMINATION OF BASIC MECHANISMS, ESTIMATION OF THE PRODUCTION RATE

S. A. Zhdanok, I. F. Buyakov,
A. V. Krauklis, and K. O. Borisevich

UDC 536.46

Results of experimental investigations on the formation of carbon nanostructures in a reactor as a result of the decomposition of hydrocarbons in a low-temperature plasma are presented. The influence of the internal geometry of the reactor, the temperature regimes, and the relative content of a reagent and an oxidizer in the working mixture on the formation of carbon nanostructures has been investigated. It was established that ordered carbon structures are formed on the surface of a metal containing iron and nickel. Data on the production rate of the process and the content of the structured carbon in the material obtained are presented.

Keywords: carbon nanomaterials, nanotubes, nanofibres, plasma, electric discharge, decomposition of hydrocarbons, mechanism of the carbide cycle.

Introduction. At present, carbon materials containing nanostructures are finding application in new fields. The increasing demands of consumers for such materials generate a need for the development of efficient and energy-saving methods of their production.

Carbon nanostructures can be obtained by different methods: in an electric arc [1], as a result of the laser ablation of graphite [2], in the process of chemical deposition of substances in the gas phase, and so on [3, 4]. However, the majority of these methods provide a low production rate (lower than 10 g/h) and call for the formation of special conditions in the synthesis zone: a low pressure, high temperatures, and the use of a catalyst, which increases the power consumption and decreases the efficiency of the process.

In the present work we consider results of investigations on a relatively new method for obtaining of carbon nanomaterials in the low-temperature plasma.

Experimental Setup. The setup used in the present work (Fig. 1) has been developed on the basis of a low-temperature plasma generator. Its main units are 1) a plasma generator of power 30 kW with a power-supply system; 2) a plasma-chemical reactor; 3) a system for delivery of the working mixture and the plasma-forming gas (air); 4) a hardening-scrubber system; 5) a system for recycling and exhaustion of the gas phase; 6) a system for cooling of the cathode, the anode insert, and the other reactor units subjected to intense heating; 7) a system for control and diagnostics. The heating of the working mixture was provided by a direct-current plasma generator of power 30 kW with a hollow copper anode and a copper cathode with a hafnium insert. The current and voltage in the plasma generator were varied within the ranges 140–190 A and 160–200 V, respectively. Air was used as the plasma-forming gas, the flow rate of which was changed from 2 to 8 m³/h.

The plasma-chemical reactor consists of a tube of stainless steel with an inner diameter of 210 mm and a thickness of 10 mm. Inside the tube was a demontable heat-insulating cylindrical insert of stainless steel, on the inner

A. V. Luikov Heat and Mass Transfer Institute, National Academy of Sciences of Belarus, 15 P. Brovka Str., Minsk, 220072, Belarus; email: borisevich-kir@yandex.ru. Translated from *Inzhenerno-Fizicheski Zhurnal*, Vol. 82, No. 3, pp. 413–419, May–June, 2009. Original article submitted May 19, 2008.

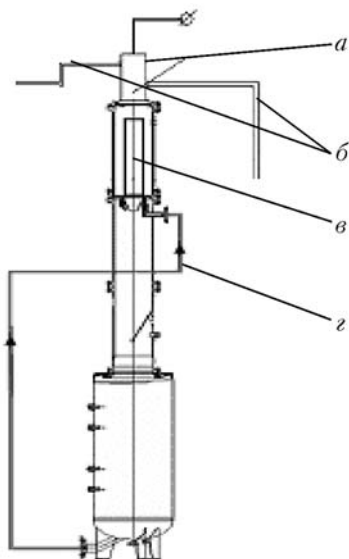


Fig. 1. Diagram of a setup for production of carbon nanomaterials in an arc discharge: a) plasma generator; b) gas system; c) plasma-chemical reactor; d) system of cooling.

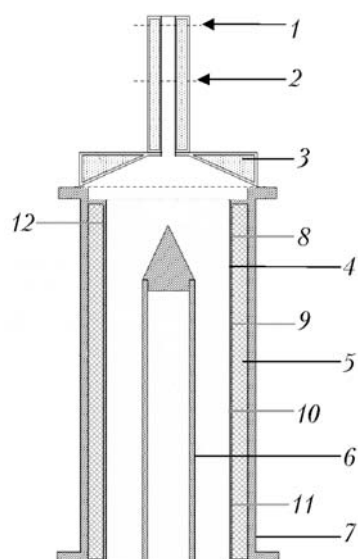


Fig. 2. Scheme of a plasma-chemical reactor: 1) supply of the plasma-forming gas; 2) supply of the working mixture; 3) cooled cover; 4) insert of the reactor; 5) thermal insulation; 6) central body; 7) outer wall of the reactor; 8–12) thermocouples (correspond to the temperatures T_1 – T_5).

surface of which carbon nanoparticles were formed. The design of the plasma-chemical reactor allowed the use of different-diameter inserts and the placement of a central body inside it (Fig. 2).

A mixture of plasma-butane with air was supplied to the plasma flow at the output of the anode. The rates of the air and gas flows were varied within the ranges 2–6 m³/h and 0.5–1.5 m³/h, respectively.

The hardening-scrubber system was designed for cooling of the working-mixture decomposition products and removal of the carbon material from the gas flow. This system includes a burner assembly, a water tank, a heat exchanger, a water pump, and a system of pipelines with a liquid filter. The water was circulated from the lower part of the water tank through the filter and the heat exchanger to the burner assembly located downstream of the plasma-chemical reactor. After the experiment, the water containing carbon particles was pumped out into special settling basins. In the water tank a gauze, on which the dense part of the suspension was deposited after the water was pumped out, was installed. Thus, in the preliminary experiments, the carbon material was taken from three different zones: the walls of the plasma-chemical reactor, the gauze of the water tank, and the suspension found in the settling basins.

The recycling system served for the possible use of the reaction products, containing methane, hydrogen, and carbon oxide, in the main process, and comprised a gas compressor, a system for dosing of the gas phase, and a unit for reclamation of the exhaust. The diagnostics and control were carried out with a system including transducers of the flow rates and pressures in the lines for supply of the working-mixture components and the plasma-forming gas and an assembly of thermocouples positioned in the regions of the plasma-chemical reactor, an analog-to-digital converter, and a personal computer with the corresponding software.

In the process of an experiment, the following parameters were measured: the temperature in different zones of the plasma-chemical reactor, the pressure and flow rates of the inward gases, the voltage and current of a discharge, and the ratio between the amounts of the reagent and the oxidizer, representing the equivalence factor γ :

$$\gamma = \frac{V_r}{V_o} n. \quad (1)$$

In the experiments, the value of γ was varied from 3 to 5.

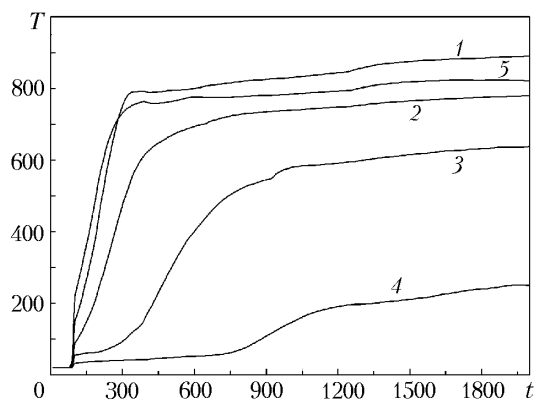


Fig. 3. Typical temperature dependences: 1–5) temperatures measured by thermocouples 8–12 in Fig. 2. T , °C; t , sec.

A mixture of the raw materials and air (the working mixture) was supplied to the air-plasma flow immediately at the output of the anode. The composition of the mixture was somewhat larger than that required for the finishing of the partial-oxidation reaction. As a result of the interaction of the working mixture with the hot plasma flow after the partial-oxidation reaction ended a mixture consisting mainly of nitrogen, hydrogen, carbon oxide, and undecomposed hydrocarbon was formed. This part of the hydrocarbon interacted with the metal of the plasma-chemical-reactor insert and, in doing so, formed carbon nanostructures. A part of the hydrocarbons was subjected to pyrolysis with formation of soot particles that were then caught in the hardening-scrubber system.

The temperature of the growth surface was 650–950°C depending on the experimental conditions and the distance between the mixture flowing to the reactor and its input. Figure 3 presents the typical change in the temperature of the process during an experiment for the case where the inner insert of the plasma-chemical reactor has the following configuration (without a central body): outer diameter, ~194 mm; inner diameter, ~190 mm; thickness of the heat-insulating layer, 10–15 mm. In this case, the flow rates of the gases involved in the process were as follows: $G_p = 5.3 \text{ m}^3/\text{h}$ for the plasma-forming gas, $G_a = 4.3 \text{ m}^3/\text{h}$ for the air in the working mixture, and $G_g = 1.7 \text{ m}^3/\text{h}$ for the gas in the working mixture. The electric power of the plasma reactor was 28 kW. As is seen from the figure, the experiment was conducted in two stages: the preliminary heating of the plasma-chemical reactor in air for 5–7 min (as long as the temperatures T_1 , T_2 , and T_5 were equal to 650–700°C) and the working regime.

After every experiment, the material was collected, cleaned, and analyzed with the use of the transmission-electron and scanning microscopy.

Results and Discussion. The preliminary investigations were conducted for the purpose of verifying the supposition that structurized carbon is contained in the material formed. As was noted above, the material taken from the three different zones was analyzed. The suspension from the settling basins and a part of the material deposited on the gauze of the water tank were preliminarily dried. The final product represented a black-gray powder with an average bulk density of $0.2 \text{ g}/\text{cm}^3$. The content of the structured carbon formed in this product was determined using of the transmission electron microscopy (TEM). Figure 4 presents photographs of the indicated material.

An analysis of the photographs of the material obtained has shown that the dry powders extracted from the suspension and from the cake on the gauze are similar in composition and mainly contain amorphous-carbon particles of different sizes (soot particles, flocs). The deposit taken from the walls of the plasma-chemical reactor contained as much as 40–50% of the structured carbon and 30% of the amorphous one. The remainder was graphite (~15%) and the particles of metals and their oxides (~5%). The material containing nanostructures was treated by a special acid and subjected to thermal processing for removal of amorphous carbon and metal particles. After the purification, the content of structured carbon was 70–80%.

The results of the preliminary experiments allow the conclusion that ordered carbon structures are formed on a metal surface containing iron and nickel, which is consistent with the idea that carbon nanomaterials are formed by the carbide-cycle mechanisms [5].

Figure 5 presents photographs of the material taken from the region of the plasma-chemical reactor; they were taken with a scanning electron microscope (SEM). It is seen that a part of carbon structures represent fibres of differ-

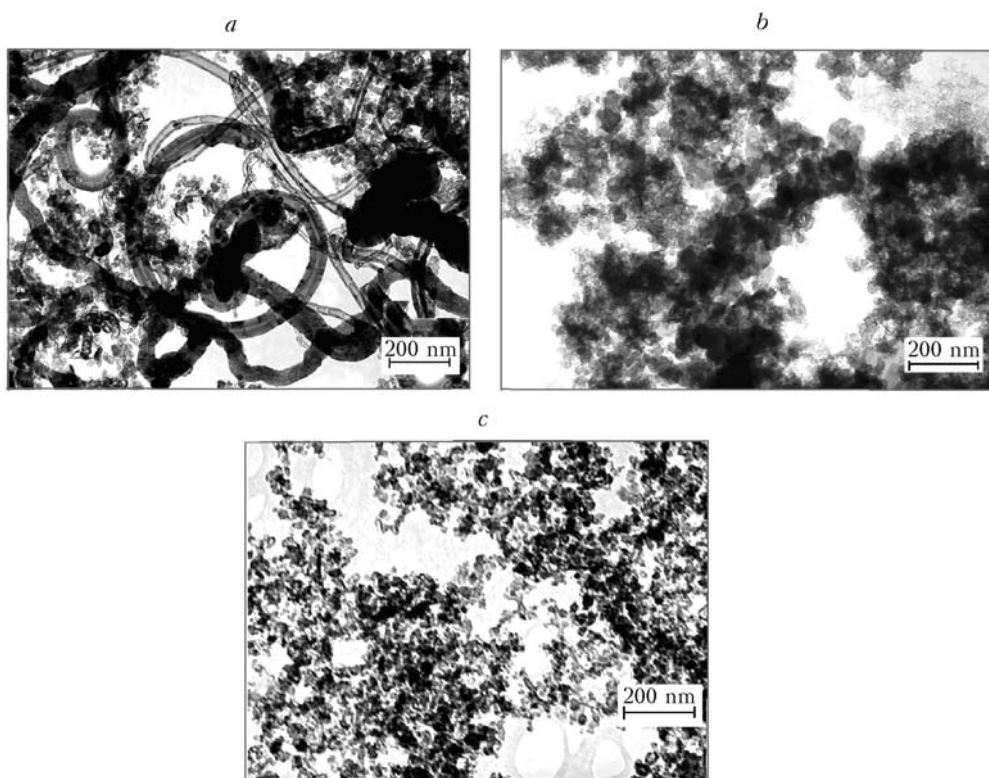


Fig. 4. TEM photographs of carbon nanomaterials: a) material formed on the walls of the plasmachemical reactor; b) material deposited on the walls of the water tank; c) material in the powder from the suspension.

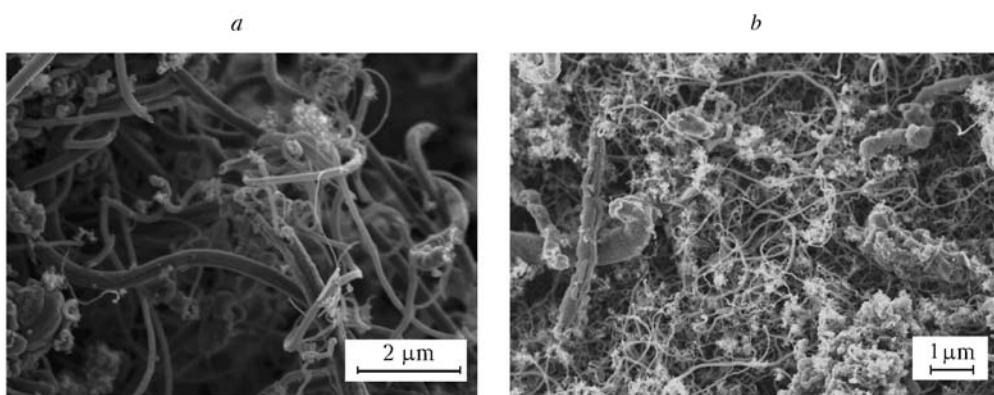


Fig. 5. SEM photographs of carbon nanomaterials formed on the walls of the plasma-chemical reactor: a) structures of large diameters; b) structures of smaller diameters.

ent length and shape with a characteristic diameter of 300 nm and larger. Moreover, the material contains structures of diameter 50–70 nm with a length of up to 1 μm that can be qualified as multiwall carbon nanotubes.

We estimated the influence of the carbon content in the working mixture, characterized by the equivalence factor γ , on the quality and quantity of the material obtained. In our experiments, the value of γ was varied from 3 to 5 at a constant flow rate ($\sim 1.5 \text{ m}^3/\text{h}$) of the propane-butane mixture. It has been established that carbon nanomaterials practically are not formed at low values of γ (as low as 3.4). When the value of γ falls within the range 3.4–3.8, a carbon material with a high content of structurized carbon ($\sim 40\text{--}50\%$) is formed on the walls of the plasmachemical reactor. The production of the deposit increases with increase in γ ; however, the degree of its structurization substan-

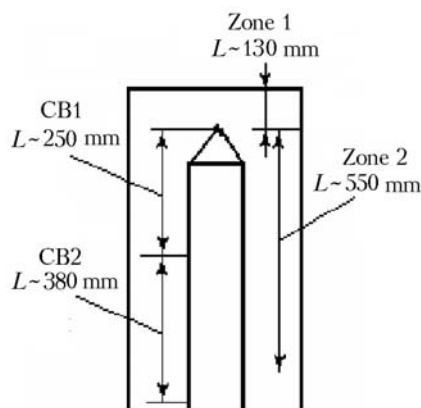


Fig. 6. Scheme of collection of the carbon deposit in the plasma-chemical reactor.

TABLE 1. Distribution of Materials over the Zones in the Reactor without a Central Body (I) and with a Central Body (II)

Material	I			II				
	Zone 1	Zone 2	All told	Zone 1	Zone 2	CB 1	CB 2	All told
Deposit, g	12.0	33.5	45.5	8.4	25.8	13.1	4.5	51.8
Nanostructures, %	30—40	30	30	30	20—30	10—20	10—20	20—30

tially decreases in this case. This is explained by the fact that the rate of growth of the carcass carbon structures in this material is actually determined by only the temperature, and, at high concentrations of hydrocarbons, an increase in the velocity of movement of carbon to the growth surface leads to the carbonization of this metal surface and the overgrowing of the carbon nanostructures with an amorphous "fur coat." Thus, in our experiments, optimum conditions for an intense growth of carbon nanostructures were realized at $\gamma \approx 3.4-3.8$.

Then we carried out experiments with the aim to investigate the possibility of increasing the production rate of the process being considered by increasing the surface, on which carbon nanostructures are formed. At the first stage, we used a central body (CB) that was positioned in the gas flow inside the plasma-chemical reactor. It represented a tube of stainless steel of length ~ 600 mm and outer diameter 96 mm with a wall of thickness 3 mm. In the experiments with the central body, an insert of inner diameter 184 mm and length ~ 680 mm with a wall of thickness 3 mm and heat-insulating layer of average thickness 10–15 mm was used in the plasma-chemical reactor. Figure 6 shows the scheme of gathering of the carbon deposit, and Table 1 presents relations between the average amounts and qualities of the materials obtained in the zones of the reactor in the experiments of half an hour's duration with the central body and without it (at $\gamma \sim 3.7$ and $t \sim 30$ min). The areas of the insert and the central body with a cone were 0.39 and 0.18 m², respectively.

In the case where the reactor operated with the central body, the specific rates of production of carbon nanomaterials on the walls of the plasmachemical reactor and the central body were 175.4 and 195.6 g/(m²·h), respectively, and the degree of structurization comprised 30–40% and 10–20%. The data presented show that the placement of the central body inside the reactor increased the rate of production of the deposit by approximately 12%; however, the relative content of the structured carbon forms in the total amount of the deposit decreased in this case.

The decrease in the structural-carbon content can be due to, first, the rapid carbonization of the metal surface of the central body, caused by the carbon contained in a large amount in the central region of the flow, and, second, the small temperature gradient between the flow and the metal surface of the central body, determining the growth of the nanostructure framework. To decrease the effect of the above-indicated factors, we proposed to use a central body consisting of two steel plates of thickness 8 mm, welded to a flange (Fig. 7). It is believed that the placement of thick plates aside of the center of the flow and an increase in the outflow of heat through them and the massive flange will make it possible to provide the required temperature gradient. However, in our experiments the degree of structurization of the carbon nanomaterials obtained on the metal plates did not exceed 10–15%, even though the specific rate of

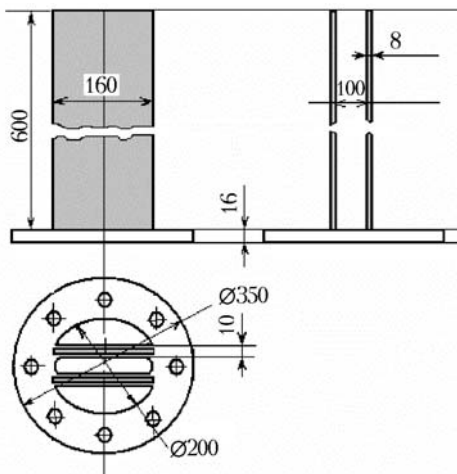


Fig. 7. Inner insert in the plasma-chemical reactor.

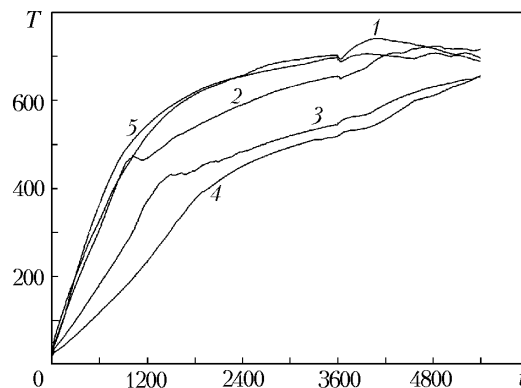


Fig. 8. Typical temperature dependences of the process in the reactor with a new insert (designations 1–5 are identical to those in Fig. 3): diameter, 200 mm; length, 680 mm; wall thickness, 10 mm. T , °C; t , sec.

production of this material was on the average 200–250 g/(m²·h). This means that there is no point in using additional surfaces in the reactor being considered for the purpose of increasing the growth of carbon nanostructures.

Another possibility of increasing the production rate of the indicated setup is to enlarge the area of the growth surface and provide optimum conditions for the growth. As the curves presented in Fig. 3 show, the temperature of a large part of the surface of the plasma-chemical-reactor insert in the region of the fourth thermocouple does not exceed 300°C during the working period, which is insufficient for an effective growth of carcass carbon structures. For this reason a different insert with thicker walls has been fabricated. It was believed that this will make it possible to increase the heat conduction of the insert and, by this means, to provide a heat transfer from its high-temperature zone to the "cold" part. Figure 8 presents typical temperature dependences for different zones of the plasma-chemical reactor with a new insert. It is seen that, even in the time interval where the process is nonstationary, the temperature of the "cold" part of the insert reaches 500–600°C. In this case, the specific rate of production of the material on the plasma-chemical-reactor wall increased to 250 g/(m²·h) and the production rate of the setup reached 100 g/h at an average structurization of the material of up to 40%.

Conclusions. Our experimental investigations have shown that, in the process of treatment of an air-hydrocarbon mixture in a reactor, carbon nanomaterials are formed on its steel surface by analogy with the catalytic decomposition of hydrocarbons by the carbide-cycle mechanism. The influence of different parameters of this process (the equivalence factor, the temperature, the internal geometry of the reactor) on the formation of carbon nanomaterials and the rate of their production was determined. In the case where the setup being investigated operated under optimum conditions, the rate of production of carbon nanomaterials reached 100 g/h at a structured-carbon content of up to 40%. The material obtained was analyzed. Further investigations in this direction will be devoted to solving the problem of increasing the efficiency of the process being considered and prevention of a deterioration of the quality of the material in the process of a prolonged continuous operation of the setup.

NOTATION

G_a , air-flow rate in the working mixture, m³/h; G_g , flow rate of a gas (reagent), m³/h; G_p , flow rate of the plasma-forming gas, m³/h; n , stoichiometrical coefficient; T , temperature, °C; t , experimental time, min; γ , equivalence factor (stoichiometrical ratio); ν_r , ν_o , number of moles. Subscripts: a, air; g, gas; p, plasma-forming; r, reagent; o, oxidizer.

REFERENCES

1. M. Cadek, R. Murphy, B. McCarthy, A. Drury, B. Lahr, and R. C. Barklie, Optimization of the arc-discharge production of multi-walled carbon nanotubes, *Carbon*, **40**, 923–928 (2002).
2. S. Arepalli, P. Nikolaev, W. Holmes, and S. Bradley, Production and measurements of individual single-wall nanotubes and small ropes of carbon, *Appl. Phys. Lett.*, **78**, No. 10, 1–3 (2001).
3. P. Chen, X. Wu, J. Lin, H. Li, and K. L. Tan, Comparative studies on the structure and electronic properties of carbon nanotubes prepared by the catalytic pyrolysis of CH₄ and disproportionation of CO, *Carbon*, **38**, 139–143 (2000).
4. N. A. Kiselev, J. L. Hutchison, A. P. Moravsky, E. V. Rakova, E. V. Dreval, C. J. D. Hetherington, D. N. Zakharov, J. Sloan, and R. O. Loutfy, Carbon micro- and nanotubes synthesized by PE-CVD technique: Tube structure and catalytic particles crystallography, *Carbon*, **42**, 149–161 (2004).
5. R. A. Buyanov and V. V. Chesnokov, On the processes proceeding in metal particles in the catalytic decomposition of hydrocarbons on them by the carbide-cycle mechanism, *Khim. Interes. Ustoich. Razv.*, No. 13, 37–40 (2005).
6. M. A. Ermakova, D. Yu. Ermakov, A. L. Chuvilin, and G. G. Kuvshinov, Decomposition of methane over iron catalysts at the range of moderate temperatures: The influence of structure of the catalytic systems and the reaction conditions on the yield of carbon and morphology of carbon filaments, *J. Catal.*, **201**, 183–197 (2001).